

Gene silencing in the marine diatom *Phaeodactylum tricornutum*

Valentina De Riso¹, Raffaella Raniello¹, Florian Maumus², Alessandra Rogato¹,
Chris Bowler^{2,3} and Angela Falciatore^{1,*}

¹Laboratory of Ecology and Evolution of Plankton, Stazione Zoologica Anton Dohrn, Villa Comunale, 80121, Napoli, Italy, ²CNRS UMR 8186, Department of Biology, Ecole Normale Supérieure, 46 rue d'Ulm, 75005, Paris, France and ³Stazione Zoologica Anton Dohrn, Villa Comunale, 80121, Napoli, Italy

Received November 11, 2008; Revised May 6, 2009; Accepted May 12, 2009

ABSTRACT

Diatoms are a major but poorly understood phytoplankton group. The recent completion of two whole genome sequences has revealed that they contain unique combinations of genes, likely recruited during their history as secondary endosymbionts, as well as by horizontal gene transfer from bacteria. A major limitation for the study of diatom biology and gene function is the lack of tools to generate targeted gene knockout or knockdown mutants. In this work, we have assessed the possibility of triggering gene silencing in *Phaeodactylum tricornutum* using constructs containing either anti-sense or inverted repeat sequences of selected target genes. We report the successful silencing of a *GUS* reporter gene expressed in transgenic lines, as well as the knockdown of endogenous phytochrome (*DPH1*) and cryptochrome (*CPF1*) genes. To highlight the utility of the approach we also report the first phenotypic characterization of a diatom mutant (*cpf1*). Our data open the way for reverse genetics in diatoms and represent a major advance for understanding their biology and ecology. Initial molecular analyses reveal that targeted downregulation likely occurs through transcriptional and post-transcriptional gene silencing mechanisms. Interestingly, molecular players involved in RNA silencing in other eukaryotes are only poorly conserved in diatoms.

INTRODUCTION

Diatoms are successful unicellular algae that arose at least 180 million years ago following a secondary

endosymbiotic event and that assimilate at least 20% of CO₂ on the planet (1,2). The molecular basis for their ecological success is largely unknown. Recently, analysis of whole genome sequences from *Thalassiosira pseudonana* (3,4) and *Phaeodactylum tricornutum* (5) indicate that these organisms have particular metabolic pathways and other unique features that might partially explain their extraordinary adaptation to a very wide range of habitats and environmental conditions. For example, they contain not only genes encoding typical components of photosynthesis but also genes encoding components typical of animal cells, never found previously in a photosynthetic eukaryote (3). Diatoms have also recruited an enormous number of genes by horizontal gene transfer from prokaryotes, and many are likely to provide novel possibilities for metabolite management and for the perception of environmental signals (5). Comparative analyses of the two diatom genomes indicate major differences in genome structure, and a substantial fraction of diatom specific genes of unknown function (around 40%), whose characterization represents a major challenge for the comprehension of diatom biology (5).

Due to the ecological significance of diatoms and their potential in helping to dissect the evolution of eukaryotes, efforts have been made in recent years to develop molecular techniques based on nuclear transformation (6,7), genome-enabled resources such as comprehensive EST libraries (<http://www.biologie.ens.fr/diatomics/EST3/>) (8,9), and whole genome microarrays (10). Nevertheless, a major limitation for the study of diatom gene function is the lack of tools to generate knockout or knockdown mutants through forward or reverse genetic approaches. The generation of loss-of-function mutants by insertional mutagenesis appears difficult in a diploid organism such as *P. tricornutum* that may lack a sexual cycle. As there is no evidence for homologous recombination events in diatoms (11), it is also unlikely that targeted gene disruption

*To whom correspondence should be addressed. Tel: +39 081 5833268; Fax: +39 081 7641355; Email: afalciat@szn.it

The authors wish it to be known that, in their opinion, the first two authors should be regarded as joint First Authors.

© 2009 The Author(s)

This is an Open Access article distributed under the terms of the Creative Commons Attribution Non-Commercial License (<http://creativecommons.org/licenses/by-nc/2.0/uk/>) which permits unrestricted non-commercial use, distribution, and reproduction in any medium, provided the original work is properly cited.

via homologous recombination can be developed as a standard approach.

In the last decade, ~20–30-nt RNA molecules generated by double-stranded RNA (dsRNA) precursors have been found to act as novel regulators of gene expression by participating in different RNA silencing processes that are collectively referred to as RNA-mediated interference (RNAi) (12–15). This regulation can drastically affect genome function, e.g. by affecting chromatin structure, transcription, RNA processing, RNA stability and translation (16,17). RNAi has also emerged as an extremely powerful tool for functional genomic analyses in many organisms. For a long time, one method to interfere with expression of a target gene had been the stable transformation of constructs expressing a gene or gene fragment in the anti-sense orientation (18,19). Subsequently, the discovery that the ultimate trigger for gene silencing was double-stranded RNA revealed that this process can be enhanced by simultaneous sense and anti-sense expression or by the direct production of high levels of dsRNA from inverted repeat constructs. Although exogenously triggered RNA silencing remains one of the least understood silencing systems (13), in the last years many attempts have been made to improve the technology (20–23), and to define optimal knockdown constructs for stable, efficient and high-throughput gene silencing in plants and animals (24–27).

In this report, we have investigated the possibility of achieving gene silencing in the diatom model species *P. tricornutum* by introducing constructs that express anti-sense or inverted-repeat containing RNAs. We show that a *GUS* reporter gene expressed in a transgenic line can be successfully silenced using both types of constructs, revealing for the first time the presence of a functional silencing machinery in diatoms and demonstrating the feasibility of targeted gene knockdown in these organisms. Additionally, we show that expression of two endogenous *P. tricornutum* genes, encoding phytochrome (Dph1) and cryptochrome/photolyase family 1 (CPF1), can also be modulated using a similar approach. A detailed *in silico* analysis of the diatom genomes for known components of the RNAi pathway indicates that molecular players involved in RNA silencing in other eukaryotes are only poorly conserved in diatoms, and that distantly related proteins may fulfil their function in these organisms.

MATERIALS AND METHODS

Cell culture

The CCMP632 strain of *P. tricornutum* Bohlin was obtained from the Provasoli-Guillard National Center for Culture of Marine Phytoplankton. Cultures were grown in f/2 medium (28) at 18°C under white fluorescent lights ($70 \mu\text{mol m}^{-2} \text{s}^{-1}$), 12 h:12 h dark–light cycle. Analyses of the wild-type and knockdown mutants have been performed on cells in exponential phase of growth and collected simultaneously, 4 h after the beginning of the light period.

Gene silencing vectors

GUS, *Dph1* and *CPF1* silencing vectors were generated and introduced in *P. tricornutum* as described in Supplementary Data.

GUS assay

Histochemical assays were performed on cells grown on plates (11). For spectrophotometric assays, a cell pellet corresponding to 5×10^7 cells was resuspended in 120 μl *GUS* extraction buffer (50 mM NaP pH 7, 10 μM β -mercaptoethanol, 0.1% Triton X-100), twice frozen and thawed and finally centrifuged at 15000g for 5 min at 4°C. *GUS* assays were performed by incubating 10 μg of total protein extract with the substrate p-nitrophenyl glucuronide (PNPG) at 1 mM final concentration. After a 2-h incubation at 37°C, the reaction was stopped by adding 0.4 ml 2.5 M 2-amino-2methyl-1,3 propanediol and absorbance was measured at 415 nm. Enzymatic activity was calculated on the basis of the OD recorded and the molar extinction coefficient of the *GUS* substrate p-nitrophenol (29). The percentage of *GUS* activity in the silenced clones was normalized with the activity in the Pt/*GUS* strain (100% activity).

Gene expression and protein analyses

RNA extraction and quantitative real time-PCR (qRT-PCR) were performed on wild-type cells and on the *GUS*, *DPH1* and *CPF1* silenced lines as described in Supplementary Data and (6). Proteins were extracted and analysed by western blotting as described in Supplementary Data.

DNA methylation analyses

McrBC PCR. Genomic DNA (600 ng) was digested overnight at 37°C with the *McrBC* enzyme (BioLabs), which requires GTP as cofactor. The presence of methylated sites was verified by performing a PCR on the *GUS* gene. As negative control, the same amplification reaction was performed on DNA digested with *McrBC* without GTP. Different fragments were amplified by PCR: the 5' fragment of the *GUS* gene, corresponding to the first 998 bp, using the primers *1Gusfw* and *Guslrw*; the 3' fragment, covering the 945–1807-bp sequence with primers *3Gusfw* and *4Gusrv*; the promoter and terminator regions, amplified with primers *FcpBfw* and *Gusrv1*, and *5Gusfw* and *FcpArv*, that yield 600-bp and 240-bp products, respectively. As an independent control, the full-length *CPF1* of 2000 bp was amplified with primers *Cpf1fw* and *Cpf1rv*. For primer sequences see Supplementary Data.

Bisulfite sequencing. Genomic DNA from the fir-1 RNAi clone was treated with bisulfite using the MethylCode Bisulfite Conversion Kit (Invitrogen). The converted DNA was subsequently amplified by PCR with AccuPrime™ Taq DNA Polymerase (Invitrogen) using a combination of primers for sense and anti-sense amplification of the *FcpBp-GUS-FcpA3'* region (Supplementary Data). PCR products were cloned in pCR2.1

vectors using TA cloning kit (Invitrogen) and transformed into TOP10 *Escherichia coli*. Positive colonies were identified by PCR, and products were subsequently sequenced. From each pair of primers, 8–12 reads were then aligned with the fir-1 construct using ClustalW to identify methylated (unconverted) cytosine residues.

UV damage response

Different dilutions of wild-type and *cpf1* mutant cells (3×10^5 , 2.5×10^5 , 1.5×10^5 and 1.25×10^5 cells) were spotted on f/2 agar plates. Cells were irradiated with UV light at 100 J/m^2 using an UV Stratalinker (Stratagene) and were then transferred under white light to promote photoreactivation. Plates inoculated in an identical manner but without UV exposure were used as control. Cell survival after UV exposure was monitored after 1 week of growth under normal light conditions. Experiments were repeated three times with similar results.

Sequence and phylogenetic analyses

We examined the *P. tricornutum* and *T. pseudonana* nuclear genomes for the presence of genes encoding RNAi components as described in Supplementary Data. The phylogenetic tree of Ago-Piwi family proteins was constructed with the AGO-PIWI domain using the Neighbor Joining method with the Mega 4 platform (30).

RESULTS AND DISCUSSION

Silencing of a *GUS* reporter gene in *P. tricornutum*

In order to establish a gene silencing methodology for diatoms we first targeted a reporter gene expressed in a transgenic line, as has been done in other organisms (31,32). We specifically used β -glucuronidase (*GUS*) because *GUS* activity can be easily detected and quantified in diatoms (Figure 1A) (11).

Due to the pioneering nature of the work, different constructs were generated containing either anti-sense or inverted repeat fragments of the *GUS* gene (Figure 1B). To increase the number of silenced transformants and to make the screening more efficient, we cloned the *GUS* fragments as part of a transcriptional fusion downstream of the selectable *Sh ble* gene, which confers resistance to the antibiotic phleomycin (11). To drive transcript expression, we tested two different *P. tricornutum* promoters, FcpBp and H4p, from the Fucoxanthin Chlorophyll *a/c*-binding Protein B and a Histone H4 gene, respectively. The FcpB promoter is routinely used to obtain strong expression of transgenes in *P. tricornutum* (33,34) and the H4p, although weaker, has been recently identified as a good candidate to drive constitutive expression (6). To determine whether anti-sense RNA length could also affect silencing efficiency, we generated different anti-sense constructs containing *GUS* fragments of 240 and 390 bp. The constructs containing the inverted repeat *GUS*

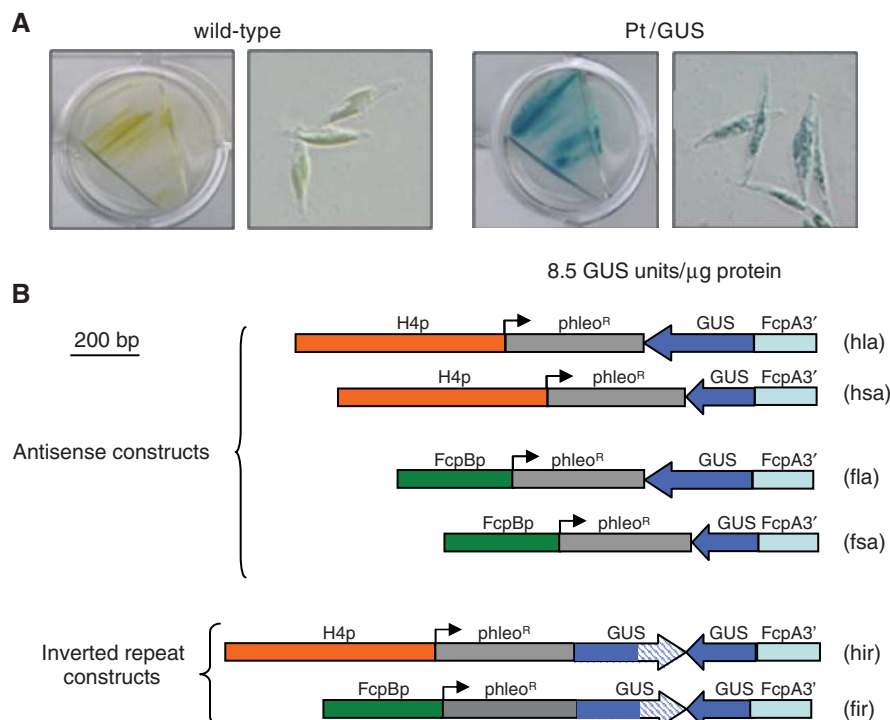


Figure 1. (A) Wild-type (left) and transgenic *P. tricornutum* cells (right) expressing the *GUS* gene, grown on agar plates and stained for *GUS* activity. Groups of cells are shown in blow up. *GUS* activity in the Pt/*GUS* strain used for the silencing analysis is indicated. (B) Schematic maps of the antisense and the inverted repeat constructs. Anti-sense constructs: *GUS* fragments of 240 or 390 bp cloned between the stop codon of the selectable *Sh ble* gene and the diatom FcpA terminator region. Inverted-repeat constructs: the *GUS* fragments were cloned in sense and anti-sense orientation. The region of self-complementarity is shown in blue, whereas the non-complementary region (corresponding to the spacer) is indicated by the diagonal lines. H4p (Histone 4 promoter), FcpBp (Fucoxanthin Chlorophyll *a/c*-binding Protein B promoter).

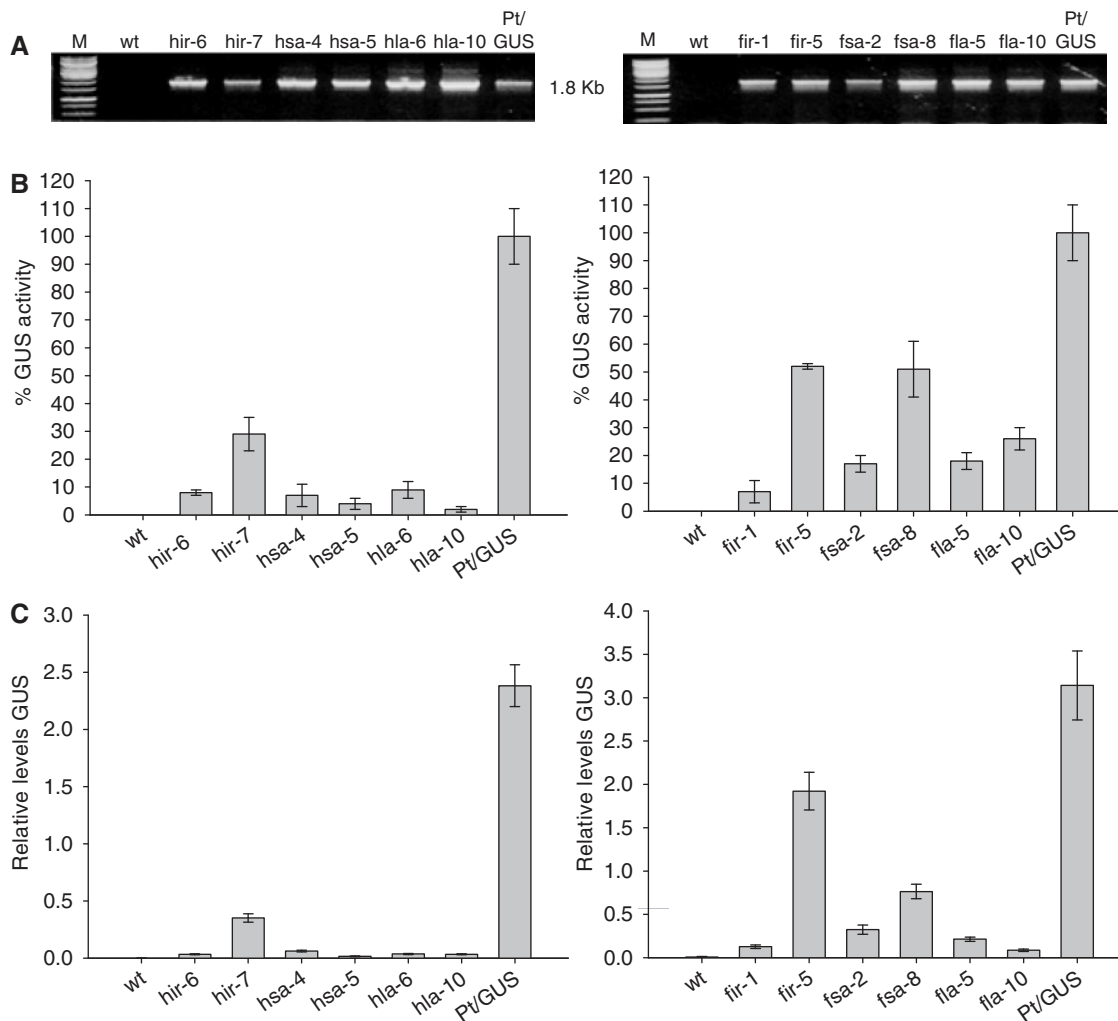


Figure 2. Molecular analysis of silenced clones. (A) PCR analysis of the full length *GUS* gene in the untransformed wild-type strain (wt), in the transgenic *GUS* expressing cells (Pt/*GUS*), and in selected silenced clones. M, 1 Kb DNA size marker. (B) *GUS* activity of the clones shown in (A). Values are normalized to the mean *GUS* activity of the Pt/*GUS* strains (100% activity). Pt/*GUS* data are the mean of 10 independent sub-clones from the *GUS* parental transgenic strain. (C) Relative *GUS* mRNA levels analysed by qRT-PCR in the same strains, and normalized with respect to the expression of an internal standard *RPS* gene.

fragments were expected to encode for RNAs that fold into hairpin structures. As it has been shown that the presence of a spacer between the self-complementary components increases the stability of the hairpin structure (35), we cloned a long sense fragment and a shorter anti-sense fragment, complementary only for 240 bp and generating a loop of 150 bp after annealing (Figure 1B).

The different constructs were introduced in a transgenic *P. tricornutum* line expressing the *GUS* reporter gene (Pt/*GUS*) and putative transformants expressing the silencing construct were first selected on phleomycin. A preliminary screening of *GUS* expression levels performed by histochemical assays indeed indicated that around 50% of clones displayed a reduced *GUS* staining (data not shown). We therefore initiated a more detailed analysis by randomly selecting 10 independent antibiotic resistant clones as well as 10 sub-clones from the parental Pt/*GUS* strain. In each case, the presence of the full-length *GUS* gene was verified by PCR, and the level of *GUS* activity quantified (Figure 2 and Supplementary Table 1).

Using both anti-sense and inverted repeat constructs driven by the *FcpB* promoter, at least five clones out of 10 showed significantly reduced *GUS* activity compared to the parental strain (Supplementary Table 1). With the inverted repeat constructs (*fir*) two clones showed a level of *GUS* activity below 25% and three others around 50%. Similar results were obtained with the anti-sense short fragment (*fsa*), while the long anti-sense fragment (*fla*) had an even more pronounced effect, with nine clones out of 10 displaying *GUS* activity equal or lower than 25% of the parental strain (Supplementary Table 1). Fewer phleomycin resistant clones were obtained with the H4 promoter. Nevertheless, more than half of the transformants showed a significant reduction in *GUS* activity: with the inverted repeat constructs (*hir*), two clones displayed *GUS* activity levels close to 50% of the parental strain, and four others below 25% (Supplementary Table 1). With the H4p anti-sense constructs, PCR-analysis revealed loss of the *GUS* transgene in 6 out of 20 transformants, likely occurring before and

independently of the transformation event. These clones were not considered in further analyses. However, of the remaining clones, six displayed at least 4-fold reduction of GUS activity with the short fragment (hsa), and two with the long fragment (hla). In contrast, independent sub-clones from the parental Pt/GUS strain did not exhibit significant reduction in GUS activity over time (Figure 2 and Supplementary Table 1).

Taken together, the percentage of clones with reduced GUS activity was significant. Both anti-sense and inverted repeat constructs driven by FcpB or H4 promoters appeared to be similarly effective in repressing transgene expression, in contrast with what is observed in higher plants and in animals, where constructs containing both sense and anti-sense components are generally more efficient than those containing a single gene fragment (36,37). Further analyses using different GUS anti-sense and inverted repeat fragments and different target genes (transgene and endogenous) will be necessary to assess the generality of this unexpected result.

Silencing stability

We performed GUS assays on the resistant clones after 1 month and after 1 year to test silencing stability. For the clones used for molecular analysis, the assay was repeated every 2 months. As shown in Supplementary Table 1, the level of GUS activity did not change after 1 month and most of the clones examined maintained similar GUS activities even after 1 year, indicating that silencing was stable. However, a few clones (13%) recovered GUS activity similar to that of the parental strain after 10 months or 1 year, indicating a loss of the phenomenon. As the clones were maintained under antibiotic selection and the transgenes were still stably integrated in the genome (data not shown), it is likely that silencing was lost at a step downstream of transgene expression or that the silencing construct got silenced itself through expression of *GUS* transgene mRNA. We did not observe any clear difference in silencing stability with the inverted repeat or anti-sense constructs, or with different promoters driving expression of the transgenes.

Molecular analysis of clones with reduced GUS activity

Amplification of the full-length *GUS* gene in almost all the clones analysed indicated that the reduction in GUS activity was not due to loss of the transgene (Figure 2A and Supplementary Table 1). The integrity of the regulatory promoter and terminator regions was also confirmed by Southern blot analysis (Supplementary Figure S1). To investigate whether the attenuation of GUS activity was the result of reduced *GUS* mRNA levels, we selected two clones from each transformation series for qRT-PCR analysis. As shown in Figure 2C, steady-state levels of the *GUS* transcript were reduced to an extent that correlated with GUS activity. These results clearly indicated that for the tested constructs, *GUS* gene silencing is associated with a reduction in transcript abundance.

As yet uncharacterized factors such as transgene copy number or site of integration in the genome might explain

the observed variability in the silencing level, as also shown in other organisms (38–40).

To exclude that reduction in *GUS* transcript could result from a general inhibition of gene expression by dsRNAs, the mRNA levels of four different genes (*actin*, *ubiquitin*, *cdkA* and *RPS*) were analysed by qRT-PCR. This revealed no significant variation between the Pt/GUS parental strain and selected clones, indicating that reduction in *GUS* mRNA level is specifically triggered by the silencing constructs (Supplementary Figure S2). Additionally, we also quantified GUS activity in 10 independent Pt/GUS clones transformed with an unrelated dsRNA construct. This was achieved using an *hir* construct that is able to functionally target the diatom *NOA* gene (34) for downregulation (Rogato, A. and Falcatore, A., unpublished). None of the *hir*:NOA transformants showed a significant reduction in GUS activity (Supplementary Figure S3A and B). The reported minor variations might be due to residual nonspecific transgene silencing or to variation in transgene expression during subcloning or to the indirect effect of *NOA* gene silencing, since it is known that this gene plays a role in the modulation of stress responses (34).

De novo cytosine methylation is associated with *GUS* transgene silencing

Since it has been shown that exogenously synthesized dsRNAs can inhibit the expression of a specific gene of interest by triggering post-transcriptional mRNA cleavage, we searched for the presence of small RNAs complementary to the *GUS* transcript using standard procedures (31). Based on preliminary data, we were not able to detect fragments of 20–30 nt in the silenced clones (data not shown), although we cannot exclude that the methods for identification of these molecules need to be optimized in diatoms.

Small RNAs can also trigger transcriptional gene silencing (TGS) associated with DNA modification and chromatin remodelling (41,42). We therefore investigated the appearance of DNA methylation within the *GUS* gene of silenced clones using the McrBC methylation-restriction system (Figure 3A). The parental transgenic line did not show any difference in amplification of the *GUS* gene after McrBC treatment. By contrast, in silenced clones the partial or total failure to amplify the *GUS* gene from McrBC-treated genomic DNA indicated that the gene was indeed methylated. Reduction in PCR amplification was observed for the 5' region (PCR2) and for the 3' region (PCR3). As both the anti-sense and inverted-repeat constructs were only complementary to the 3' end of the *GUS* gene, these results suggested a spreading of methylation along the gene sequence. Consequently, we also checked for possible methylation of the promoter and terminator regions of the chimeric *GUS* gene (PCR1 and 4, Figure 3A). While reduced amplification products were observed using primers specific for the terminator sequence (PCR4), no differences with the parental Pt/GUS strain were detected when amplifying the FcpBp promoter, suggesting that only the transcribed region was modified in the silenced clones.

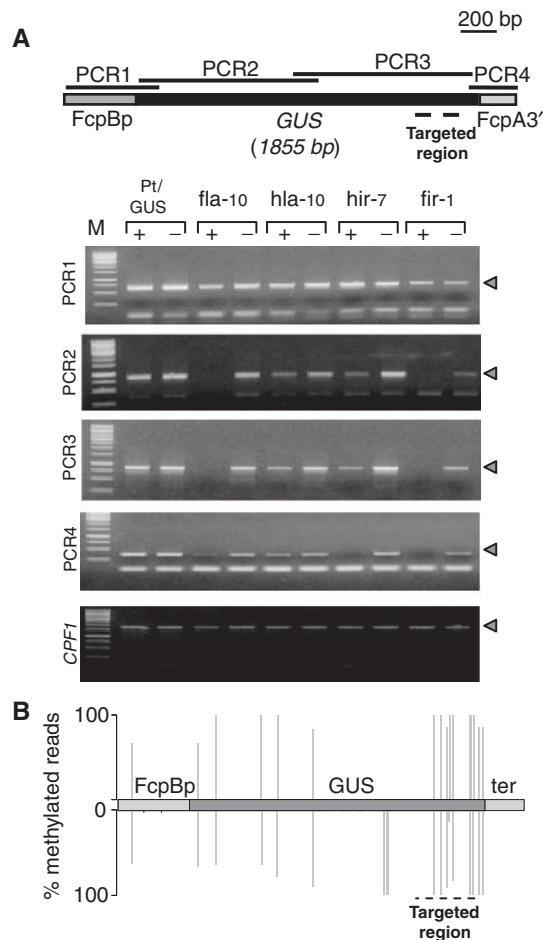


Figure 3. *De novo* cytosine methylation in silenced clones. Methylation analysis performed on the Pt/GUS expressing cells, and on selected silenced clones. (A) PCR amplifications performed on genomic DNA digested with McrBC, in the presence (+) and absence (-) of GTP, using primer sets specific for the *GUS* transgene and its regulatory regions. PCR analysis shows the amplification of the FcpBp region (PCR1), amplification of the first (PCR2) and second (PCR3) half of the *GUS* gene, the terminator region (PCR4), and amplification of the *CPF1* gene used as control. Arrows indicate the bands corresponding to the expected amplification products. M, 1-kb DNA size marker. Schematic representation of the genomic region used for the analysis and the region targeted for silencing is indicated above. (B) Schematic representation of the methylation profile obtained by bisulfite sequencing of the *fir-1* clone. Vertical bars show the distribution of mC in the sense and anti-sense strands. The targeted region is indicated.

We subsequently used bisulfite sequencing to quantify cytosine methylation and to characterize methylation profiles in the *fir-1* line. The analysis confirmed DNA methylation in the silenced line, revealing a total of 17 mC, all in a CG context, 15 of them being found symmetrically on both sense and anti-sense strands, while two were found only on the anti-sense strand (Figure 3B). Six of these sites were located in the silencing region. Cytosine methylation was also found outside of this region, with three mCs located immediately downstream and the remaining sites spreading further upstream up to the promoter. Introduction of the silencing vector in the *GUS* expressing line therefore caused *de novo* DNA methylation within the targeted region as well as methylation spreading along

the transcribed region, as also observed in plants (43,44). It thus seems that the production of dsRNAs in *P. tricornutum* feeds backward to alter chromatin structure at the level of DNA regions with which they share sequence identity by the process called RNA-directed DNA methylation (RdDM) (45). No cytosine methylation at CHG or CHH sites was found, suggesting that RNAi-induced *de novo* methylation in *P. tricornutum* may occur only in the CG context.

All together, these results indicate that in silenced clones, generated with both the anti-sense and inverted-repeat constructs, methylation marks correlate with transcriptional (or post-transcriptional) silencing of the *GUS* transgene. Although more analysis will be required to characterize the small RNAs and effector proteins putatively associated with this phenomenon, computational analyses revealed the presence of putative DNA methyltransferase genes (DMT) likely implicated in both *de novo* and maintenance cytosine methylation (data not shown). Interestingly, one of these encodes a bacterial DNMT1 orthologue. Association of cytosine methylation to transgene silencing is of particular interest since it has also been found in the sequences of diatom transposable elements, likely implicated in the control of their mobility under stress (Maumus, F. *et al.*, submitted). This might suggest the presence of a surveillance system against foreign DNAs that might act through chromatin-targeted RNAi, as shown in other organisms (14).

Silencing of the endogenous *P. tricornutum* *DPH1* and *CPF1* genes

In order to test whether endogenous genes could also be silenced, we attempted to knockdown the expression of two putative photoreceptors identified in the *P. tricornutum* genome: the phytochrome (Dph1) and cryptochrome/photolyase family protein 1 (CPF1). Different vectors containing inverted repeat sequences from the *DPH1* and *CPF1* genes were generated. To drive *DPH1* silencing, a vector whose expression was under control of the FcpBp was tested (*fir-Dph1*), whereas vectors containing the *FcpB* or the *H4* promoters were constructed for *CPF1* down-regulation (*fir-CPF1* and *hir-CPF1*) (Figure 4A and B). The targeted regions corresponded to the 5' and 3' regions, respectively, of *DPH1* and *CPF1* (Figure 4C and D). Putative silenced clones were screened by immunoblot for decreased Dph1 and CPF1 content using specific antisera generated in the laboratory. From a total of 70 transgenic clones, six displayed reduced amounts of Dph1 protein, ranging between 25 and 50% of wild-type levels. Three of these clones (*dph1-1*, *dph1-2* and *dph1-3*) are shown in Figure 4E. For CPF1, from a total of 50 transformants, five displayed protein levels between 10 and 30% of wild-type levels. The use of the *H4* and *FcpB* promoters gave similar results: two of the silenced clones were obtained from screening 28 transformants containing the vector *fir-CPF1* (clones *cpf1-1* and *cpf1-2* in Figure 4F) and three from a screen of 22 transformants containing vector *hir-CPF1* (*cpf1-3* in Figure 4F). These data are the first to show silencing of endogenous diatom genes, and confirm a silencing efficiency of around 10%.

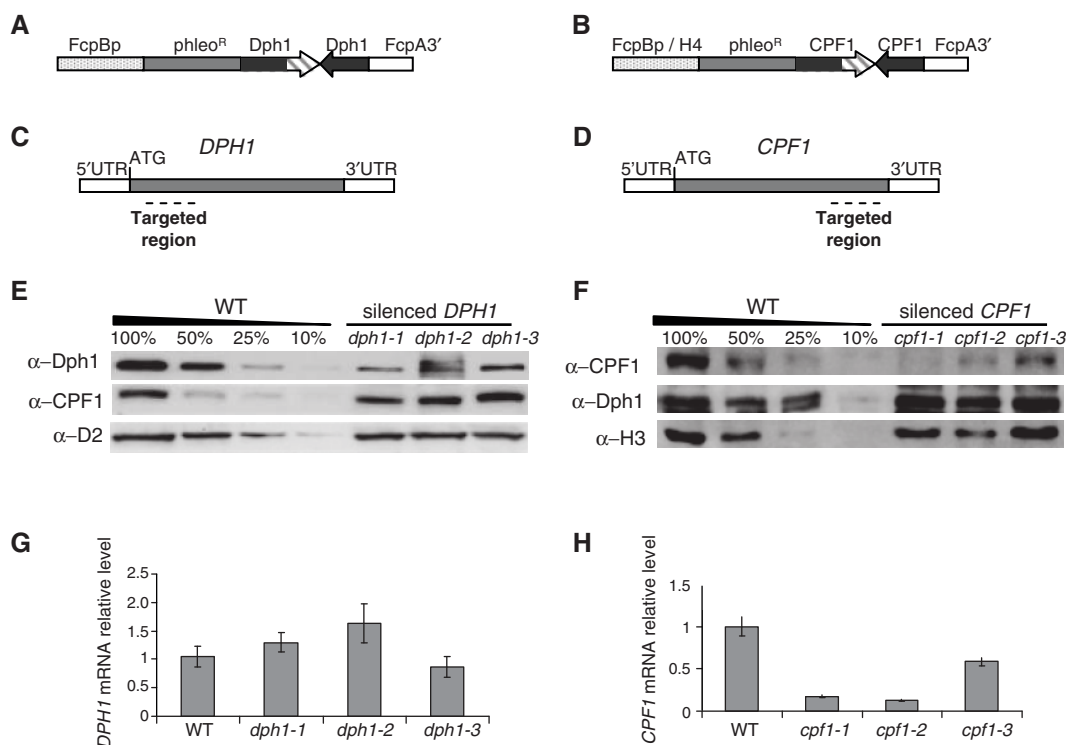


Figure 4. Silencing of endogenous *DPH1* and *CPF1*. (A and B) Schematic representation of the fir-Dph1 and fir-CPF1 constructs used for transformation. (C and D) Schematic representation of *DPH1* and *CPF1* targeted regions. (E and F) Analysis of Dph1 and CPF1 protein levels by immunoblot in independent silenced lines (clones *dph1-1* to *dph1-3*, and clones *cpf1-1* to *cpf1-3*). Dph1 and CPF1 protein levels were quantified using a serial dilution of proteins from wild-type cells as standard. The same membranes were incubated with D2, and histone H3 antibodies as loading control, respectively. (G and H) *DPH1* and *CPF1* mRNA levels in the silenced clones quantified by qRT-PCR. Normalization was done relative to *RPS* mRNA.

CPF1 silencing was stronger than that observed for *DPH1*. This could possibly be due to the different target regions. However, other factors such as sequence composition, spatial and temporal gene expression patterns, and RNA turnover rates of the targeted gene might affect silencing effectiveness (46).

As diatoms are routinely grown under light/dark cycles and *CPF1* expression is moderately induced by light (47), we wanted to test silencing stability under different light conditions. Results shown in Supplementary Figure S4 indicate that CPF1 protein content could be reduced to non-detectable levels in dark-adapted cells. Light-induction of the *CPF1* gene by 3-h light treatment could nonetheless stimulate the appearance of some protein, which might correspond to residual levels of *CPF1* mRNA accumulation when the silencing machinery has to compete against increased gene expression. The fir-CPF1 vector seemed slightly more efficient in maintaining silencing after the light shift. Since it is known that the *FcpB* gene is light induced (6), it is likely that expression of the silencing construct under FcpBp might also increase following the light treatment.

Cross-hybridization using both antibodies showed that the reduction in protein levels was specific for each targeted gene (Figure 4E and F). Each protein also accumulated to wild-type levels in a silenced Pt/GUS transgenic line and in Pt/GUS transformed with an unrelated hir construct for *NOA* gene silencing, showing the

specificity of targeted down-regulation (Supplementary Figure S3).

Surprisingly, analysis of *DPH1* and *CPF1* mRNA levels by qRT-PCR gave strikingly opposite effects: while *CPF1* mRNA was reduced to an extent that correlates with protein abundance, *DPH1* mRNA exhibits a normal, if not elevated, level as compared to wild-type (Figure 4G and H). Remarkably, analysis of *P. tricornutum* cells silenced in other endogenous genes such as *NOA* also revealed normal transcript levels (data not shown). Altogether the data suggest the existence of two possible silencing mechanisms based on transcriptional and/or mRNA slicing for the *GUS* transgene and the *CPF1* endogene, while *DPH1* downregulation might be affected through translation inhibition. Further characterization of these lines and the possible identification of small RNAs will help deciphering silencing mechanisms in marine diatoms.

cpf1 phenotype analysis

Recently the biochemical characterization of *P. tricornutum* CPF1 revealed that this protein is a novel blue-light sensor displaying DNA repair activity. Additional analysis in diatoms over-expressing *CPF1* demonstrated that the protein also acts as a transcriptional regulator (47). We therefore performed a phenotypic characterization of the *cpf1* knockdown mutant by testing UV sensitivity. As shown in Figure 5A, *cpf1-1* showed substantially reduced survival after exposure to UV compared to the

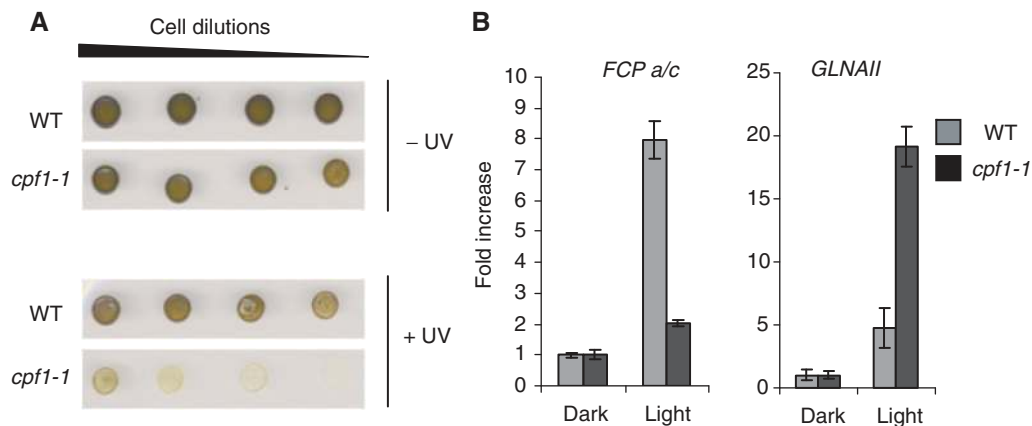


Figure 5. Effect of *CPF1* downregulation on UV damage response and light-induced gene expression. (A) *cpf1-1* growth defect after UV-C irradiation. Dilution series of wild-type and *cpf1-1* cells were grown for 1 week after exposure to UV light at 100 J/m^2 . (B) Analysis of *FCP a/c* and *GLNAII* mRNA levels in 60-h dark-adapted cultures and then exposed for 5 min to $3.3\ \mu\text{mol m}^{-2}\text{ s}^{-1}$ of blue light. Relative transcript levels were determined by qRT-PCR using *RPS* as a reference gene. Values were normalized to gene expression levels in the dark.

wild type, thus confirming a role in repair of UV damage. Moreover, a role in blue-light regulated gene expression was also verified by checking the expression of genes encoding fucoxanthin chlorophyll *a/c*-binding protein (*FCP a/c*) and glutamine synthetase (*GLNAII*) in dark-adapted cells exposed to a 5-min pulse of low-intensity blue light (Figure 5B). The results indicated that the expression of the *FCP a/c* gene was significantly dampened in the knockdown mutant compared to the wild type, whereas expression of the *GLNAII* was enhanced. By contrast, opposite responses were reported in the over-expressing lines (47). These analyses represent the first phenotypic characterization of a diatom knock-down mutant demonstrating the utility of the approach for gene function studies.

Identification of genes encoding putative components of the RNAi machinery in diatom genomes

The successful demonstration of *GUS*, *CPF1* and *DPH1* gene silencing prompted us to examine the available diatom genome sequences for genes encoding putative components of the RNAi machinery identified in other organisms. In particular we searched for genes encoding putative Dicer, Argonaute-Piwi and RNA-dependent RNA polymerase (RdRP), key RNAi components already present in the last common eukaryotic ancestor and that have significantly expanded and diversified in multicellular eukaryotes (48). These core components are also present in unicellular eukaryotes with relatively large genomes such as *Chlamydomonas reinhardtii*, but not in green and red unicellular algae with small nuclear genomes (49), suggesting an independent loss of the machinery during eukaryotic evolution.

Dicer homologues, which process dsRNA precursors to small RNA molecules of $\sim 21\text{--}24$ nt, typically contain an amino-terminal DEADc/HELICASEc domain, followed by a domain of unknown function (DUF283), a PAZ domain, two neighbouring RNase III domains (RNase IIIa and RNase IIIb), and a double-stranded

RNA-binding domain (dsRBD) (Figure 6A). Previous analysis in the diatom genomes indicated the absence of a canonical Dicer in these organisms. However, this overall gene structure organization does not apply to all organisms. For instance, the Dicer-like protein 1 (DCL1) from the ciliate protozoan *Tetrahymena thermophila* (a chromalveolate) only contains the two RNase III domains and a dsRBD domain (50). The *Giardia intestinalis* (an excavate) DCL1 (51) consists of a PAZ domain, a divergent DUF283 motif and two adjacent RNase III domains. Remarkably, the highly divergent *Trypanosoma brucei* (another excavate) Dicer-like 1, which contains only two RNase III domains, drives the RNA interference pathway in this organism (52). Therefore, to date, the only universal feature of the Dicer family is the presence of two RNase III domains. We thus searched both diatom genomes for candidate gene models matching these criteria. In the *T. pseudonana* genome we found a gene model encoding a protein with two RNase III domains (Tp3_11638) and in *P. tricornutum* another (Pt2_48138) containing a dsRBD followed by two RNase III domains (Figure 6A and Supplementary Table S2). Therefore, putative diatom Dicer-like proteins are only distantly related to the multi-domain proteins identified in plants and animals, although the conservation in terms of domain structure and key amino acid residues with other eukaryotes (Supplementary Figure S5A) (53), particularly from chromalveolates, may support their role as *bona fide* Dicercs.

Interestingly, we identified an additional gene model (Tp3_20605) in the *T. pseudonana* genome that may play a role in RNA silencing (Supplementary Table S2). This protein displays a domain association that we could not find in any other organism, consisting of a DEADc/HELICASEc followed by a C-terminal dsRBD. The DEAD/HELICASEc domain from this protein has homology with the DEAD/HELICASEc domains in a range of Dicer-like proteins.

The Argonaute proteins, core components of the effector RNA-induced silencing complexes (RISC), are classified into three paralogous groups: the Argonaute-like

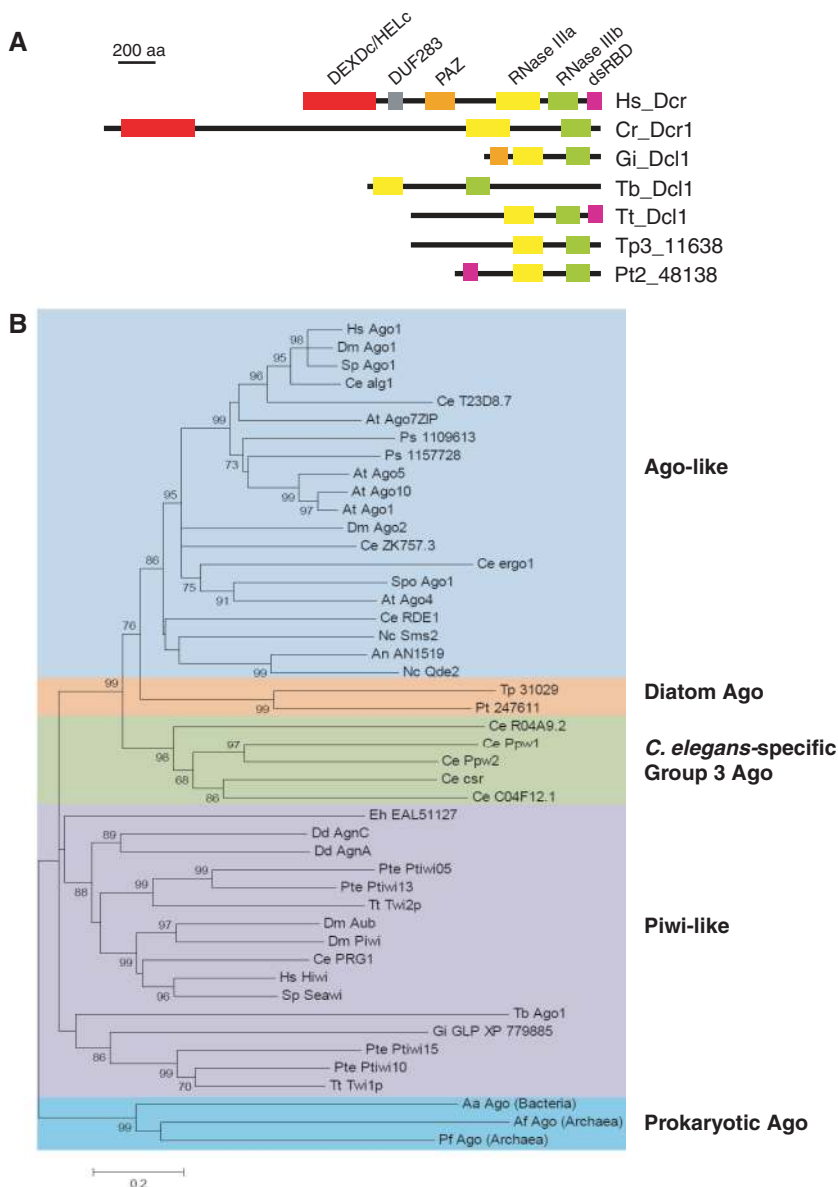


Figure 6. Possible candidates for diatom Dicer-like and AGO-like RNAi components. (A) Schematic representation of domains found in various Dicer (Dcr) and Dicer-like (Dcl) proteins. Domain abbreviations: *DEXDc/HELIC*, DEAD-like helicase domain/helicase C-terminal domain; *DUF283*, DUF283 domain; *PAZ*, PAZ domain; *RNaseIII (a-b)*, ribonuclease III domains a and b and dsRBD, double-stranded RNA-binding domain. Species abbreviations: Cr, *Chlamydomonas reinhardtii*; Gi, *Giardia intestinalis*; Hs, *Homo sapiens*; Pt, *Phaeodactylum tricornutum*; Tb, *Trypanosoma brucei*; Tp, *Thalassiosira pseudonana*; Tt, *Tetrahymena thermophila*. (B) Phylogenetic analysis of the diatom Argonaute-like proteins. Phylogenetic tree constructed using the MEGA 4.0 platform with the Neighbor-Joining method from a MUSCLE alignment of the PAZ and AGO domains from Ago-like, Piwi-like, *Caenorhabditis elegans*-specific group 3 Argonautes, prokaryotic Argonautes, and the putative diatom Ago-Piwi-like proteins identified in this work. The alignment was manually refined to remove gaps and erroneous positions. Numbers indicate interior branch bootstrap values as percentage, based on 1000 pseudoreplicates (only values >60% are shown). Species abbreviations and accession numbers of proteins used to draw the tree: Aa, *Aquifex aeolicus* (AA Ago gi126031218); Af, *Archaeoglobus fulgidus* (Af Ago gi60593831); An, *Aspergillus nidulans* (AN1519, EAA63775); At, *Arabidopsis thaliana* (At Ago1 AAC18440, At Ago4 NP565633, At Ago5 NP850110, At Ago7 ZIP NP177103, At Ago10 CAA11429); Ce, *C. elegans* (CeC04F12.1 gi17505468, Ce ZK757.3 gi17557077, Ce R04A9.2 gi17569229, Ce PRG1 gi3875393, Ce T23D8.7 gi3880077, Ce RDE1 gi6272678, Ce Alg1 gi25148113, Ce csr1 gi115532838, Ce ergo1 gi25148583, Ce ppw1 NP740835, Ce ppw2 AAF60414); Dd, *Dictyostelium discoideum* (Dd AgnA EAL69296, Dd AgnC EAL71514); Dm, *Drosophila melanogaster* (Dm Ago1 BAA88078, Dm Ago2 Q9VUQ5, Dm Aub CAA64320, Dm Piwi Q9VKM1); Eh, *Entamoeba histolytica* (Eh EAL51127); Gi, *G. intestinalis* (Gi GLP XP779885); Hs, *H. sapiens* (Hs Ago1 AAH63275, Hs Hiwi AAC97371); Nc, *Neurospora crassa* (Nc Qde2 AAF43641, Nc Sms2 AAN32951); Pf, *Pyrococcus furiosus* (Pf Ago gi62738878); Pte, *Paramecium tetraurelia* (Pte Ptiwi05 CA144468, Pte Ptiwi10 CA139070, Pte Ptiwi13 CA139067, Pte Ptiwi15 CA139065); Sp, *Strongylocentrotus purpuratus* (Sp Ago1 XP782278, Sp Seawi AAG42533); Spo, *Saccharomyces pombe* (Ago1 O74957); Tb, *T. brucei* (Ago1 O74957); Tt, *T. thermophila* (Tt Twi1p AAM77972, Tt Twi2p AAQ74967); Ps, *Phytophthora sojae* (1109613, 1157728); Pt, *P. tricornutum* (FJ750269); Tp, *T. pseudonana* (FJ750270).

(AGO-like) proteins, similar to *Arabidopsis thaliana* AGO1, the Piwi-like proteins, related to the *Drosophila melanogaster* PIWI, and the recently identified *Caenorhabditis elegans*-specific group 3 Argonautes (15). Animals have retained members of both the AGO-like and Piwi subfamilies, whereas the different Argonautes identified in green algae and plants all belong to the AGO-like subfamily (15,54). The Argonaute proteins involved in RNAi pathways always contain distinct functional domains: a variable N-terminal domain and conserved C-terminal PAZ, MID and PIWI domains (15). The PIWI domain often has endonuclease activity, although this activity is not essential for RNAi regulation function. Putative proteins containing these domains were identified both in *T. pseudonana* (Tp3_1029) and *P. tricornutum* (Pt2_47611; Supplementary Table S2). Multiple alignment of the Ago-Piwi domain from diatoms with other Ago-Piwi proteins revealed significant conservation, although the catalytic site for endonuclease activity was only poorly conserved (55) (Supplementary Figure S5B). Phylogenetic analysis of the diatom Argonautes with proteins identified in other eukaryotes revealed that they cluster together in a clade only distantly related to the known paralogous groups mentioned above (Figure 6B), suggesting a possible functional specialization.

In some eukaryotes, RdRPs are also involved in the silencing process (56). By generating dsRNA from single-stranded transcripts, RdRP may be involved in the initiation of RNAi or in the amplification of the response by increasing the amount of dsRNA (48). We found a gene encoding putative RdRP in *P. tricornutum* (Pt2_45417) and two in *T. pseudonana* (Tp3_8685 and Tp3_5028; Supplementary Table S2).

Recently, analysis of diatom genomes has revealed an extraordinary combination of novel genes with the potential to encode innovative metabolisms (5). Additionally, phylogenetic analysis of *P. tricornutum* genes indicates that at least 5% of the genome is derived from bacterial orthologues, an unusually high number for a eukaryote (5). Thus, besides the proteins described above and reported in Supplementary Table S2, it is likely that novel proteins and protein complexes, perhaps also of prokaryotic origin, are involved in the RNA regulation and related silencing processes described in this work. The functional and biochemical characterization of diatom silencing complexes will therefore be of great interest and will be necessary to decipher the key components of the silencing machinery in these organisms.

CONCLUSIONS

In this work, we have demonstrated the feasibility of establishing gene silencing in the model diatom *P. tricornutum*. A range of different constructs was first tested to trigger *GUS* transgene silencing and to provide evidence for the effectiveness of the methodology. Subsequently, inverted-repeat vectors were also used to successfully suppress expression of the endogenous *DPH1* and *CPF1* genes. A significant reduction in endogenous targeted protein content was observed in different

transgenic lines, and the first phenotype resulting from gene knockdown in a marine eukaryotic phytoplankton organism has been reported. Together with the two genome sequences that are now available, the possibility of dissecting gene function through reverse genetics represents a major advance for understanding diatom biology and the mechanisms underlying the success of these organisms in the oceans. The recent development of a transformation system for *T. pseudonana* (57) opens the way for targeted gene silencing in this diatom as well, and in the absence of other gene inactivation approaches we expect that the technique reported here will become widely employed.

The initial characterization of the silenced clones presented in this work strongly supports the presence of functional gene silencing pathways in diatoms, acting through inhibitory transcriptional and post-transcriptional mechanisms. Notwithstanding, *in silico* characterization of non-canonical components of the RNAi machinery (specifically Dicer-like and RISC machinery) and the initial molecular analysis of knockdown mutants also indicate a possible diversification of the underlying silencing mechanisms. Thus, deciphering the diatom RNAi machinery will now be necessary to characterize the RNAi components proposed in this work and to assess the presence of silencing-induced small RNAs. Remarkably, endogenous small non-coding RNAs (and putative miRNAs) have been recently identified in *P. tricornutum* by small-RNA library sequencing (Hess, W., Voss, B. and Falciatore, A., unpublished data). Hence, marine diatoms also represent an attractive model to study evolution and differentiation of RNAi mechanisms in eukaryotes.

SUPPLEMENTARY DATA

Supplementary Data are available at NAR Online.

ACKNOWLEDGEMENTS

We thank Alessandra De Martino for providing the parental transgenic lines expressing *GUS*, the Molecular Biology Service (Stazione Zoologica, Naples) for assistance with qRT-PCR, Maria Grazia Adelfi for mutant screening, Alessandro Manfredonia for culture preparation, and Frédy Barneche and Martine Boccara (Ecole Normale Supérieure, Paris) for critical suggestions.

FUNDING

The Human Frontier Science Program-CDA (0014/2006) to A.F.; the Agence Nationale de la Recherche (France); to C.B.; the EU-FP6 Marine Genomics Network of Excellence (GOCE-CT-2004-505403); and the EU-funded FP6 Diatomics project (LSHG-CT-2004-512035). Funding for open access charge: Human Frontier Science Program-CDA (0014/2006).

Conflict of interest statement. None declared.

REFERENCES

1. Falkowski, P.G., Barber, R.T. and Smetacek, V.V. (1998) Biogeochemical controls and feedbacks on ocean primary production. *Science*, **281**, 200–207.
2. Smetacek, V. (1999) Diatoms and the ocean carbon cycle. *Protist*, **150**, 25–32.
3. Armbrust, E.V., Berges, J.A., Bowler, C., Green, B.R., Martinez, D., Putnam, N.H., Zhou, S., Allen, A.E., Apt, K.E., Bechner, M. *et al.* (2004) The genome of the diatom *Thalassiosira pseudonana*: ecology, evolution, and metabolism. *Science*, **306**, 79–86.
4. Montsant, A., Andrew, E.A., Coesel, S., De Martino, A., Falcitore, A., Heijde, M., Jabbari, K., Maheswari, U., Mangogna, M., Rayko, E. *et al.* (2007) Identification and comparative genomic analysis of signaling and regulatory mechanisms in the diatom *Thalassiosira pseudonana*. *J. Phycol.*, **43**, 585–604.
5. Bowler, C., Allen, A.E., Badger, J.H., Grimwood, J., Jabbari, K., Kuo, A., Maheswari, U., Martens, C., Maumus, F., Otiillar, R.P. *et al.* (2008) The Phaeodactylum genome reveals the evolutionary history of diatom genomes. *Nature*, **456**, 239–244.
6. Saut, M., Heijde, M., Mangogna, M., Montsant, A., Coesel, S., Allen, A., Manfredonia, A., Falcitore, A. and Bowler, C. (2007) Molecular toolbox for studying diatom biology in *Phaeodactylum tricornutum*. *Gene*, **406**, 23–35.
7. Kroth, P.G. (2007) Genetic transformation: a tool to study protein targeting in diatoms. *Methods Mol. Biol.*, **390**, 257–267.
8. Montsant, A., Jabbari, K., Maheswari, U. and Bowler, C. (2005) Comparative genomics of the pennate diatom *Phaeodactylum tricornutum*. *Plant Physiol.*, **137**, 500–513.
9. Maheswari, U., Mock, T., Armbrust, E.V. and Bowler, C. (2009) Update of the Diatom EST Database: a new tool for digital transcriptomics. *Nucleic Acids Res.*, **37**, D1001–D1005.
10. Mock, T., Samanta, M.P., Iverson, V., Berthiaume, C., Robison, M., Holtermann, K., Durkin, C., Bondurant, S.S., Richmond, K., Rodesch, M. *et al.* (2008) Whole-genome expression profiling of the marine diatom *Thalassiosira pseudonana* identifies genes involved in silicon bioprocesses. *Proc. Natl Acad. Sci. USA*, **105**, 1579–1584.
11. Falcitore, A., Casotti, R., Leblanc, C., Abrescia, C. and Bowler, C. (1999) Transformation of nonselectable reporter genes in marine diatoms. *Marine Biotech.*, **1**, 239–251.
12. Baulcombe, D. (2004) RNA silencing in plants. *Nature*, **431**, 356–363.
13. Brodersen, P. and Voinnet, O. (2006) The diversity of RNA silencing pathways in plants. *Trends Genet.*, **22**, 268–280.
14. Chapman, E.J. and Carrington, J.C. (2007) Specialization and evolution of endogenous small RNA pathways. *Nat. Rev. Genet.*, **8**, 884–896.
15. Hutvagner, G. and Simard, M.J. (2008) Argonaute proteins: key players in RNA silencing. *Nat. Rev. Mol. Cell Biol.*, **9**, 22–32.
16. Carthew, R.W. and Sontheimer, E.J. (2009) Origins and mechanisms of miRNAs and siRNAs. *Cell*, **136**, 642–655.
17. Voinnet, O. (2009) Origin, biogenesis, and activity of plant microRNAs. *Cell*, **136**, 669–687.
18. Nellen, W. and Lichtenstein, C. (1993) What makes an mRNA anti-sense-itive? *Trends Biochem. Sci.*, **18**, 419–423.
19. van der Krol, A.R., Mol, J.N. and Stuitje, A.R. (1988) Antisense genes in plants: an overview. *Gene*, **72**, 45–50.
20. Lamitina, T. (2006) Functional genomic approaches in *C. elegans*. *Methods Mol. Biol.*, **351**, 127–138.
21. Dykxhoorn, D.M., Novina, C.D. and Sharp, P.A. (2003) Killing the messenger: short RNAs that silence gene expression. *Nat. Rev. Mol. Cell Biol.*, **4**, 457–467.
22. Montgomery, M.K. (2004) RNA interference: historical overview and significance. *Methods Mol. Biol.*, **265**, 3–21.
23. Hope, I.A. (2001) Broadcast interference – functional genomics. *Trends Genet.*, **17**, 297–299.
24. Schroda, M. (2006) RNA silencing in *Chlamydomonas*: mechanisms and tools. *Curr. Genet.*, **49**, 69–84.
25. Watson, J.M., Fusaro, A.F., Wang, M. and Waterhouse, P.M. (2005) RNA silencing platforms in plants. *FEBS Lett.*, **579**, 5982–5987.
26. Li, L., Lin, X., Khvorova, A., Fesik, S.W. and Shen, Y. (2007) Defining the optimal parameters for hairpin-based knockdown constructs. *RNA*, **13**, 1765–1774.
27. Ramadan, N., Flockhart, I., Booker, M., Perrimon, N. and Mathey-Prevot, B. (2007) Design and implementation of high-throughput RNAi screens in cultured *Drosophila* cells. *Nat. Protoc.*, **2**, 2245–2264.
28. Guillard, R.R.L. (1975) Culture of phytoplankton for feeding marine invertebrates. In Smith, W.L. and Chanley, M.H. (eds), *Culture of Marine Invertebrate Animals*, New York, USA, pp. 29–60.
29. Jefferson, R.A., Kavanagh, T.A. and Bevan, M.W. (1987) GUS fusions: beta-glucuronidase as a sensitive and versatile gene fusion marker in higher plants. *EMBO J.*, **6**, 3901–3907.
30. Tamura, K., Dudley, J., Nei, M. and Kumar, S. (2007) MEGA4: Molecular Evolutionary Genetics Analysis (MEGA) software version 4.0. *Mol. Biol. Evol.*, **24**, 1596–1599.
31. Hamilton, A.J. and Baulcombe, D.C. (1999) A species of small antisense RNA in posttranscriptional gene silencing in plants. *Science*, **286**, 950–952.
32. Jones, L., Hamilton, A.J., Voinnet, O., Thomas, C.L., Maule, A.J. and Baulcombe, D.C. (1999) RNA-DNA interactions and DNA methylation in post-transcriptional gene silencing. *Plant Cell*, **11**, 2291–2301.
33. Apt, K.E., Kroth-Pancic, P.G. and Grossman, A.R. (1996) Stable nuclear transformation of the diatom *Phaeodactylum tricornutum*. *Mol. Gen. Genet.*, **252**, 572–579.
34. Vardi, A., Bidle, K.D., Kwitny, C., Hirsh, D.J., Thompson, S.M., Callow, J.A., Falkowski, P. and Bowler, C. (2008) A diatom gene regulating nitric-oxide signaling and susceptibility to diatom-derived aldehydes. *Curr. Biol.*, **18**, 895–899.
35. Smith, N.A., Singh, S.P., Wang, M.B., Stoutjesdijk, P.A., Green, A.G. and Waterhouse, P.M. (2000) Total silencing by intron-spliced hairpin RNAs. *Nature*, **407**, 319–320.
36. Waterhouse, P.M., Graham, M.W. and Wang, M.B. (1998) Virus resistance and gene silencing in plants can be induced by simultaneous expression of sense and antisense RNA. *Proc. Natl Acad. Sci. USA*, **95**, 13959–13964.
37. Wesley, S.V., Helliwell, C.A., Smith, N.A., Wang, M.B., Rouse, D.T., Liu, Q., Gooding, P.S., Singh, S.P., Abbott, D., Stoutjesdijk, P.A. *et al.* (2001) Construct design for efficient, effective and high-throughput gene silencing in plants. *Plant J.*, **27**, 581–590.
38. Waterhouse, P.M. and Helliwell, C.A. (2003) Exploring plant genomes by RNA-induced gene silencing. *Nat. Rev. Genet.*, **4**, 29–38.
39. Brown, A.E., Bugeon, L., Crisanti, A. and Catteruccia, F. (2003) Stable and heritable gene silencing in the malaria vector *Anopheles stephensi*. *Nucleic Acids Res.*, **31**, e85.
40. Rohr, J., Sarkar, N., Balenger, S., Jeong, B.R. and Cerutti, H. (2004) Tandem inverted repeat system for selection of effective transgenic RNAi strains in *Chlamydomonas*. *Plant J.*, **40**, 611–621.
41. Zilberman, D., Cao, X. and Jacobsen, S.E. (2003) ARGONAUTE4 control of locus-specific siRNA accumulation and DNA and histone methylation. *Science*, **299**, 716–719.
42. Chan, S.W. (2008) Inputs and outputs for chromatin-targeted RNAi. *Trends Plant. Sci.*, **13**, 383–389.
43. Vaistij, F.E., Jones, L. and Baulcombe, D.C. (2002) Spreading of RNA targeting and DNA methylation in RNA silencing requires transcription of the target gene and a putative RNA-dependent RNA polymerase. *Plant Cell*, **14**, 857–867.
44. Daxinger, L., Kanno, T., Bucher, E., van der Winden, J., Naumann, U., Matzke, A.J. and Matzke, M. (2009) A stepwise pathway for biogenesis of 24-nt secondary siRNAs and spreading of DNA methylation. *EMBO J.*, **28**, 48–57.
45. Matzke, M., Kanno, T., Huettel, B., Daxinger, L. and Matzke, A.J. (2007) Targets of RNA-directed DNA methylation. *Curr. Opin. Plant Biol.*, **10**, 512–519.
46. Kerschen, A., Napoli, C.A., Jorgensen, R.A. and Muller, A.E. (2004) Effectiveness of RNA interference in transgenic plants. *FEBS Lett.*, **566**, 223–228.
47. Coesel, S., Mangogna, M., Ishikawa, T., Heijde, M., Rogato, A., Finazzi, G., Todo, T., Bowler, C. and Falcitore, A. (2009) Diatom PtCPF1 is a new cryptochrome/photolyase family member with DNA repair and transcription regulation activity. *EMBO Rep.*, May 8. [Epub ahead of print].

48. Cerutti, H. and Casas-Mollano, J.A. (2006) On the origin and functions of RNA-mediated silencing: from protists to man. *Curr. Genet.*, **50**, 81–99.
49. Casas-Mollano, J.A., Rohr, J., Kim, E.J., Balassa, E., van Dijk, K. and Cerutti, H. (2008) Diversification of the core RNA interference machinery in *Chlamydomonas reinhardtii* and the role of DCL1 in transposon silencing. *Genetics*, **179**, 69–81.
50. Mochizuki, K. and Gorovsky, M.A. (2005) A Dicer-like protein in *Tetrahymena* has distinct functions in genome rearrangement, chromosome segregation, and meiotic prophase. *Genes Dev.*, **19**, 77–89.
51. Macrae, I.J., Zhou, K., Li, F., Repic, A., Brooks, A.N., Cande, W.Z., Adams, P.D. and Doudna, J.A. (2006) Structural basis for double-stranded RNA processing by Dicer. *Science*, **311**, 195–198.
52. Shi, H., Tschudi, C. and Ullu, E. (2006) An unusual Dicer-like protein fuels the RNA interference pathway in *Trypanosoma brucei*. *RNA*, **12**, 2063–2072.
53. Blaszczyk, J., Tropea, J.E., Bubunenko, M., Routzahn, K.M., Waugh, D.S., Court, D.L. and Ji, X. (2001) Crystallographic and modeling studies of RNase III suggest a mechanism for double-stranded RNA cleavage. *Structure*, **9**, 1225–1236.
54. Vaucheret, H. (2008) Plant ARGONAUTES. *Trends Plant Sci.*, **13**, 350–358.
55. Yuan, Y.R., Pei, Y., Ma, J.B., Kuryavii, V., Zhadina, M., Meister, G., Chen, H.Y., Dauter, Z., Tuschl, T. and Patel, D.J. (2005) Crystal structure of *A. aeolicus* argonaute, a site-specific DNA-guided endoribonuclease, provides insights into RISC-mediated mRNA cleavage. *Mol. Cell*, **19**, 405–419.
56. Wassenegger, M. and Krczal, G. (2006) Nomenclature and functions of RNA-directed RNA polymerases. *Trends Plant Sci.*, **11**, 142–151.
57. Poulsen, N., Chesley, P.M. and Kroger, N. (2006) Molecular genetic manipulation of the diatom *Thalassiosira pseudonana* (Bacillariophyceae). *J. Phycol.*, **42**, 1059–1065.